CrystEngComm

PAPER

View Article Online
View Journal | View Issue

Cite this: *CrystEngComm*, 2014, **16**, 328

Metallohexacycles containing 4′-aryl-4,2′:6′,4″-terpyridines: conformational preferences and fullerene capture†

Edwin C. Constable,* Catherine E. Housecroft,* Srboljub Vujovic and Jennifer A. Zampese

Received 4th October 2013,
Accepted 30th October 2013

DOI: 10.1039/c3ce42012d

www.rsc.org/crystengcomm

4′-(4-Biphenylyl)-4,2′:6′,4″-terpyridine (**1**) reacts with $ZnCl_2$ or $ZnBr_2$ to produce discrete metallohexacycles instead of the expected one-dimensional coordination polymers. Structural determination of $[\{ZnCl_2(\mathbf{1})\}_6]$ and $[\{ZnBr_2(\mathbf{1})\}_6]$ reveals that the metallomacrocycles adopt a conformation in which the biphenyl domains are in an alternating up/down arrangement (conformer **I**). The hexamers pack into tubes; within each tube, biphenyl domains of every second hexamer are interdigitated, and these assemblies then interlock to produce a rigid architecture supported by pyridine–phenyl face-to-face contacts. π-Stacking between 4,2′:6′,4″-tpy domains operates between adjacent tubes. Reaction of $ZnCl_2$ or $ZnBr_2$ with 4′-(2′,3′,4′,5′,6′-pentafluorobiphenyl-4-yl)-4,2′:6′,4″-terpyridine (**2**) leads to $[\{ZnCl_2(\mathbf{2})\}_6]$ and $[\{ZnBr_2(\mathbf{2})\}_6]$, each crystallizing in two conformations; the centrosymmetric chair-conformer (**II**) is dominant with respect to the tub-like conformer **I**. Both conformers pack into tube assemblies, but that consisting of conformer **II** is less rigid than that of **I**. Reaction of 4′-(4-(naphthalen-1-yl)phenyl)-4,2′:6′,4″-terpyridine (**3**) with $ZnCl_2$ or $ZnBr_2$ leads to $[\{ZnX_2(\mathbf{2})\}_6]$ (X = Cl, Br) in conformer **I**; disordering of the naphthyl substituents is problematic. Assembly of the metallohexacycle in the presence of C_{60} results in the formation of the host–guest complex $[2\{ZnCl_2(\mathbf{3})\}_6{\cdot}C_{60}]{\cdot}6MeOH{\cdot}16H_2O$. The $[\{ZnCl_2(\mathbf{3})\}_6]$ units assemble into a tube-like array that mimics that observed in the parent host. In the host–guest complex, each crystallographically-ordered C_{60} is trapped between six ordered naphthyl units, three from one hexamer and three from its interdigitated partner, and the C_{60}–six-naphthyl unit sits centrally within a second $[\{ZnCl_2(\mathbf{3})\}_6]$ macrocycle. In contrast to previously described tube-like host–guest assemblies featuring fullerene entrapment, $[2\{ZnCl_2(\mathbf{3})\}_6{\cdot}C_{60}]$ is unusual in having an ordered array of C_{60} molecules present in every other available cavity, despite the fact that sterically, the 'empty' cavity could, in principle, host a C_{60} guest.

Introduction

A critical strategy in directing the assembly of discrete metallomacrocyclic complexes (metallopolygons) requires complementarity between the coordination preferences of a metal ion and the spatial relationship between the metal-binding domains of the bridging ligand.[1–4] Two general approaches are typically adopted. The first uses the coordination geometry of the metal ion to define the internal angle of the metallomacrocycle in combination with rigid-rod ligands, for example, a molecular square predetermined by the 90° angle of square planar platinum(II).[5] The second approach hinges upon the use of a ligand with a fixed internal angle. This strategy has been successfully exploited by the Newkome group to link $\{M(tpy)\}_2$ units (tpy = 2,2′:6′,2″-terpyridine) into molecular hexagons[6] by using ditopic bis(4′-substituted tpy) ligands in which the metal ion is effectively a rigid linear metal node. These two design strategies tend to produce metallomacrocycles in which the metal ions are in a roughly planar array. In contrast, judicious choice of ligands can lead to the assembly of helical or grid-like[7] macrocycles.[4] Regular assemblies can also be obtained with flexible ligands, although a degree of control is lost.

The geometrical flexibility of the zinc(II) ion (d^{10}) and its compatibility with hard donors (typically N and O) permit zinc(II) to be applied in a number of ways in multimetallic arrays. Both $\{Zn_2(O_2CR)_4\}$ and $\{Zn_4(\mu\text{-}O_2CR)_6(\mu_4\text{-}O)\}$ building blocks are well-established as nodes with predetermined directionality (linear and octahedral, respectively) in coordination polymers, networks and metal–organic frameworks

Department of Chemistry, University of Basel, Spitalstrasse 51, CH4056 Basel, Switzerland. E-mail: catherine.housecroft@unibas.ch; Fax: +41 61 267 1018; Tel: +41 61 267 1008

† Electronic supplementary information (ESI) available: Fig. S1–S6 ORTEP plots with atom labelling for the contents of the asymmetric units in the structures described in the paper. Crystallographic data for $[\{ZnCl_2(\mathbf{1/2})\}_6]{\cdot}2CHCl_3{\cdot}3MeOH{\cdot}9H_2O$. CCDC 956344–956349. For ESI and crystallographic data in CIF or other electronic format see DOI: 10.1039/c3ce42012d

(MOFs).[8–12] In contrast, combinations of mononuclear zinc(II) nodes (most commonly zinc halides) with bridging ligands containing N- or O-donors lead to a diverse range of coordination polymers and discrete complexes. Reactions of zinc(II) halides with 4,2′:6′,4″-terpyridines tend to lead to coordination polymers (Scheme 1a),[13–18] but the assembly of a metallohexacycle and polycatenated, triply interlocked metallocapsules has also been observed.[19,20] The unexpected formation of a molecular metallohexacycle (Scheme 1b) from $ZnCl_2$ and 4′-(4-ethynylphenyl)-4,2′:6′,4″-terpyridine under crystal growth conditions at ambient temperatures is not readily explained. In contrast to twelve examples of $[ZnX_2(4'\text{-}R'\text{-}4,2':6',4''\text{-tpy})]_n$ (X = halide or monodentate acetate) polymers present in the Cambridge Structural Database[21] (v. 5.34 with November 2012 updates using Conquest v. 1.15),[22] $[\{ZnCl_2(4'\text{-}(HC{\equiv}CC_6H_4)\text{-}4,2':6',4''\text{-tpy})\}_6]$ is a unique example of a metallomacrocyclic complex containing a 4,2′:6′,4″-tpy ligand. We now report that this motif is a persistent solid-state product in reactions of $ZnCl_2$ or $ZnBr_2$ with three 4′-aryl-4,2′:6′,4″-terpyridines (**1**–**3**, Scheme 2). We also describe initial studies of the host–guest chemistry of these metallohexacycles, exemplified by the formation of $[2\{ZnCl_2(\mathbf{3})\}_6{\cdot}C_{60}]$.

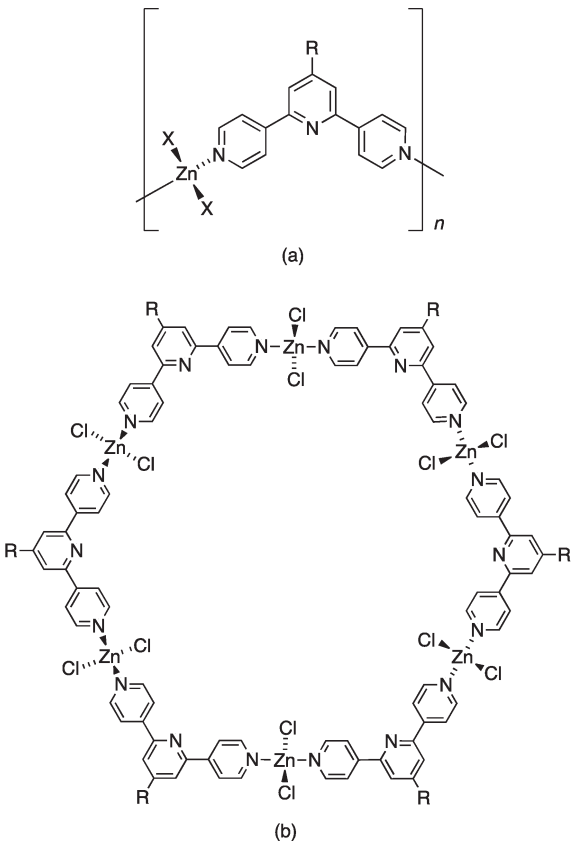

Scheme 1 (a) General structure of one-dimensional coordination polymers formed with 4′-substituted 4,2′:6′,4″-terpyridines and ZnX_2 (X = Cl, Br, I; R = various). (b) Structure of the metallohexacycle formed with $ZnCl_2$ and 4′-(4-ethynylphenyl)-4,2′:6′,4″-terpyridine (R = $HC{\equiv}CC_6H_4$); the ring has a chair conformation in the solid state.

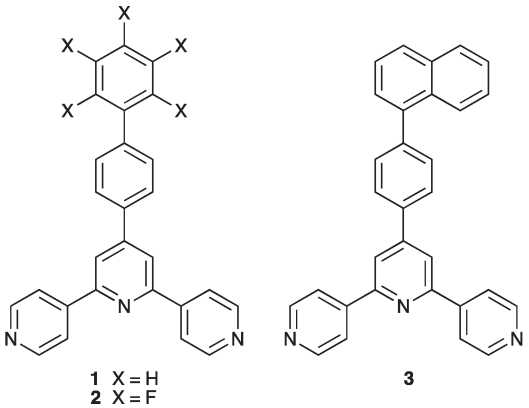

Scheme 2 Structures of ligands **1**–**3**.

Experimental section

General

Electrospray ionisation (ESI) and MALDI TOF mass spectra were measured using Bruker Esquire 3000plus and Bruker microflex instruments, respectively. Solution electronic absorption spectra were recorded using an Agilent 8453 spectrophotometer. ^{1}H NMR spectra were recorded at room temperature using a Bruker-Avance III-400 spectrometer.

Ligands **1**,[23] 224 and 325 were prepared according to literature methods.

$[\{ZnCl_2(\mathbf{1})\}_6]$

A solution of **1** (19.1 mg, 0.050 mmol) in $CHCl_3$ (6.0 mL) was placed in a long test tube. MeOH (3.0 mL) was layered on the top of the solution, followed by a solution of $ZnCl_2$ (6.76 mg, 0.050 mmol) in MeOH (5.0 mL). The test tube was sealed with parafilm and allowed to stand for 3 days at room temperature after which time, colourless crystals had formed. These were isolated by decantation (19 mg, 0.037 mmol, 73%). Found C 61.69, H 4.26, N 7.63%; $C_{162}H_{114}Cl_{12}N_{18}Zn_6{\cdot}3MeOH$ requires C 61.42, H 3.94, N 7.81%.

$[\{ZnBr_2(\mathbf{1})\}_6]$

A solution of **1** (19.1 mg, 0.050 mmol) in $CHCl_3$ (6.0 mL) was placed in a long test tube and MeOH (3.0 mL) was then layered over the first solution, followed by a solution of $ZnBr_2$ (11.2 mg, 0.050 mmol) in MeOH (5.0 mL). The tube was sealed with parafilm and left to stand at room temperature. Within 3 days, colourless crystals had formed and were isolated by decantation (10.3 mg, 0.0169 mmol, 33.7%). Found C 53.01, H 3.64, N 6.73%; $C_{162}H_{114}Br_{12}N_{18}Zn_6{\cdot}2MeOH$ requires C 52.84, H 3.30, N 6.76%.

$[\{ZnCl_2(\mathbf{2})\}_6]$

A solution of **2** (23.6 mg, 0.050 mmol) in $CHCl_3$ (6.0 mL) was placed in a long test tube and MeOH (3.0 mL) was layered over the solution. A solution of $ZnCl_2$ (6.76 mg, 0.050 mmol) in MeOH (5.0 mL) was added carefully and the tube was sealed with parafilm and left for 3 days at room temperature.

Colourless crystals (blocks and spear-like blocks) formed and were isolated by decantation (15.6 mg, 0.0255 mmol, 51.0%). Found: C 53.62, H 2.31, N 6.87%; $C_{162}H_{84}Cl_{12}F_{30}N_{18}Zn_6$ requires C 53.02, H 2.81, N 6.87%.

[{ZnBr$_2$(2)}$_6$]

A solution of 2 (23.6 mg, 0.050 mmol) in $CHCl_3$ (6.0 mL) was placed in a long tube. MeOH (3.0 mL) was layered on top of the solution, followed by a solution of $ZnBr_2$ (11.2 mg, 0.050 mmol) in MeOH (5.0 mL). The test tube was sealed with parafilm and allowed to stand for 3 days at room temperature. The colourless crystals that formed were isolated by decantation (12.7 mg, 0.0181 mmol, 36.3%). Found C 46.84, H 2.28, N 6.30%; $C_{162}H_{114}Br_{12}F_{30}N_{18}Zn_6$ requires C 46.29, H 2.01, N 6.00%.

[{ZnBr$_2$(3)}$_6$]

A solution of 3 (21.8 mg, 0.050 mmol) in $CHCl_3$ (6.0 mL) was placed in a long tube and MeOH (3.0 mL) was layered on top, followed by a solution of $ZnBr_2$ (11.2 mg, 0.050 mmol) in MeOH (5.0 mL). The test tube was sealed with parafilm and left at room temperature for 3 days. The colourless crystals that formed were isolated by decantation (13.6 mg, 0.0206 mmol, 41.2%). Found C 57.38, H 3.81, N 6.21%; $C_{186}H_{126}Br_{12}N_{18}Zn_6$ requires C 56.35, H 3.20, N 6.36%.

[2{ZnCl$_2$(3)}$_6$·C$_{60}$]

A solution of 3 (21.8 mg, 0.050 mmol) in a mixture of 1,2-$Cl_2C_6H_4$ (8.0 mL) and MeOH (2.0 mL) and a solution of C_{60} (6 mg, 0.008 mmol) in 1,2-$Cl_2C_6H_4$ (2.0 mL) were placed in a long test tube. A mixture of MeOH (2.5 mL) and 1,2-$Cl_2C_6H_4$ (2.5 mL) was added as a new layer, followed by a solution of $ZnCl_2$ (6.76 mg, 0.050 mmol) in MeOH (8 mL). After sealing the tube with parafilm, it was left for 2 weeks at room temperature. During this time, purple-red blocks formed in addition to small crystals of C_{60}. Satisfactory elemental analysis could not be obtained.

Crystallography

Single crystal data were collected on a Bruker APEX-II diffractometer with data reduction, solution and refinement using the programs APEX[26] and SHELXL97 or SHELX-13.[27] The ORTEP-type diagram and structure analysis used Mercury v. 3.0.[22,28] Rapid solvent loss and heavy disordering of solvent molecules influenced data quality in almost all structures, especially in [{ZnCl$_2$(2)}$_6$] and [{ZnBr$_2$(2)}$_6$]. Therefore, SQUEEZE[29] was used to treat the data.

[{ZnCl$_2$(1)}$_6$]·6CHCl$_3$·6MeOH·5H$_2$O

$C_{174}H_{154}Cl_{30}N_{18}O_{11}Zn_6$, M = 4129.02, colourless block, trigonal, space group $R\bar{3}$, a = b = 37.5778(11), c = 11.4003(4) Å, U = 13 941.5(8) Å^3, Z = 3, D_c = 1.472 Mg m^{-3}, μ(Mo-Kα) = 1.255 mm^{-1}, T = 123 K. Total 73 965 reflections, 9030 unique, R_{int} = 0.0423. Refinement of 6903 reflections (429 parameters) with $I > 2\sigma(I)$ converged at final R_1 = 0.0589 (R_1 all data = 0.0834), wR_2 = 0.1704 (wR_2 all data = 0.2067), gof = 1.091. CCDC 956343.

[{ZnBr$_2$(1)}$_6$]·4CHCl$_3$·5MeOH·8H$_2$O

$C_{174}H_{154}Br_{12}Cl_{12}N_{18}O_{13}Zn_6$, M = 4447.12, colourless block, trigonal, space group $R\bar{3}$, a = b = 38.1168(9), c = 11.6852(3) Å, U = 14 702.8(6) Å^3, Z = 3, D_c = 1.501 Mg m^{-3}, μ(Mo-Kα) = 3.390 mm^{-1}, T = 123 K. Total 122 861 reflections, 7121 unique, R_{int} = 0.0446. Refinement of 5926 reflections (420 parameters) with $I > 2\sigma(I)$ converged at final R_1 = 0.0333 (R_1 all data = 0.0454), wR_2 = 0.0902 (wR_2 all data = 0.1020), gof = 1.115. CCDC 956344.

[{ZnCl$_2$(2)}$_6$]·3CHCl$_3$·3MeOH·6H$_2$O (conformer I)

$C_{168}H_{111}Cl_{21}F_{30}N_{18}O_9Zn_6$, M = 4232.57, colourless block, trigonal, space group $R\bar{3}$, a = b = 37.998(4), c = 11.3178(11) Å, U = 14 152(2) Å^3, Z = 3, D_c = 1.486 Mg m^{-3}, μ(Cu-Kα) = 4.430 mm^{-1}, T = 123 K. Total 32 865 reflections, 5662 unique, R_{int} = 0.0483. Refinement of 5423 reflections (426 parameters) with $I > 2\sigma(I)$ converged at final R_1 = 0.0613 (R_1 all data = 0.0626), wR_2 = 0.1810 (wR_2 all data = 0.1826), gof = 1.051. CCDC 956347.

[{ZnCl$_2$(2)}$_6$] (conformer II)

After SQUEEZE: $C_{162}H_{84}Cl_{12}F_{30}N_{18}Zn_6$, M = 3670.71, colourless block, monoclinic, space group $P2_1/n$, a = 9.2722(4), b = 35.4234(15), c = 30.2123(12) Å, β = 95.305(2), U = 9880.8(7) Å^3, Z = 2, D_c = 1.234 Mg m^{-3}, μ(Cu-Kα) = 2.941 mm^{-1}, T = 123 K. Total 72 063 reflections, 17 471 unique, R_{int} = 0.0753. Refinement of 12 646 reflections (1182 parameters) with $I > 2\sigma(I)$ converged at final R_1 = 0.1069 (R_1 all data = 0.1240), wR_2 = 0.3013 (wR_2 all data = 0.3169), gof = 1.089. CCDC 956348.

[{ZnBr$_2$(2)}$_6$]

After SQUEEZE: $C_{162}H_{84}Br_{12}F_{30}N_{18}Zn_6$, M = 4203.61, colourless block, trigonal, space group $R\bar{3}$, a = b = 38.394(4), c = 11.5576(15) Å, U = 14 755(3) Å^3, Z = 3, D_c = 1.419 Mg m^{-3}, μ(Cu-Kα) = 4.311 mm^{-1}, T = 123 K. Total 29 568 reflections, 5754 unique, R_{int} = 0.1096. Refinement of 4031 reflections (343 parameters) with $I > 2\sigma(I)$ converged at final R_1 = 0.0769 (R_1 all data = 0.1008), wR_2 = 0.1903 (wR_2 all data = 0.2024), gof = 1.116. CCDC 956349.

[{ZnBr$_2$(3)}$_6$]·3CHCl$_3$·15H$_2$O

$C_{189}H_{159}Br_{12}Cl_9N_{18}O_{15}Zn_6$, M = 4592.60, colourless block, trigonal, space group $R\bar{3}$, a = b = 38.975(2), c = 11.4827(8) Å, U = 15 105.8(17) Å^3, Z = 3, D_c = 1.505 Mg m^{-3}, μ(Mo-Kα) = 3.264 mm^{-1}, T = 123 K. Total 125 042 reflections, 8934 unique, R_{int} = 0.0580. Refinement of 6705 reflections (585 parameters) with $I > 2\sigma(I)$ converged at final R_1 = 0.0425 (R_1 all data = 0.0703), wR_2 = 0.1267 (wR_2 all data = 0.1717), gof = 1.111. CCDC 956345.

[2{ZnCl$_2$(3)}$_6$·C$_{60}$]·6MeOH·16H$_2$O

$C_{438}H_{308}Cl_{24}N_{36}O_{22}Zn_{12}$, M = 8062.51, red block, trigonal, space group $R\bar{3}$, a = b = 38.4322(16), c = 22.5450(10) Å, U = 28 838(2) Å^3,

Z = 3, D_c = 1.387 Mg m^{-3}, μ(Mo-Kα) = 0.970 mm^{-1}, T = 123 K. Total 279 568 reflections, 17 029 unique, R_{int} = 0.0350. Refinement of 13 522 reflections (1015 parameters) with $I > 2\sigma(I)$ converged at final R_1 = 0.0638 (R_1 all data = 0.0860), wR_2 = 0.1735 (wR_2 all data = 0.2072), gof = 1.115. CCDC 956346.

Results and discussion

[{ZnCl$_2$(**1**)}$_6$] and [{ZnBr$_2$(**1**)}$_6$]

Ligand **1** reacted with $ZnCl_2$ or $ZnBr_2$ under conditions of crystal growth by layering at room temperature. Colourless blocks grew within three days and crystals with only one habit were observed in both reactions. Single crystal X-ray analysis revealed the formation of the molecular metallohexacycles [{ZnCl$_2$(**1**)}$_6$] and [{ZnBr$_2$(**1**)}$_6$] as solvates [{ZnCl$_2$(**1**)}$_6$]·6CHCl$_3$·6MeOH·5H$_2$O and [{ZnBr$_2$(**1**)}$_6$]·4CHCl$_3$·5MeOH·8H$_2$O. Both compounds crystallize in the trigonal space group $R\bar{3}$ with cell parameters that are very similar. The asymmetric unit of each structure contains one molecule of **1** and one ZnX_2 unit (X = Cl or Br, Fig. S1 and S2†) and the hexacycle is generated by 3-fold rotoinversion. Fig. 1 shows the structures of the metallocycles [{ZnCl$_2$(**1**)}$_6$] and [{ZnBr$_2$(**1**)}$_6$]. The two views illustrate the alternating up/down arrangement of the ligands (labelled conformer **I**), and this contrasts with the three-up/three-down arrangement (corresponding to a chair conformation) observed in [{ZnCl$_2$(**4**)}$_6$] (**4** = 4′-(4-ethynylphenyl)-4,2′:6′,4″-terpyridine).[19] We return to the question of ring conformation later. In each complex, the Zn atom is tetrahedrally sited and, as is typical of 4,2′:6′,4″-terpyridines, only the outer pyridine rings of ligand **1** are involved in coordination. Bond parameters within the zinc(II) coordination spheres in solvated [{ZnCl$_2$(**1**)}$_6$] and [{ZnBr$_2$(**1**)}$_6$] are given in Table 1. The tpy domain in each complex deviates slightly from planarity (angles between the rings containing N1/N2 and N2/N3 = 5.5 and 14.2° in [{ZnCl$_2$(**1**)}$_6$], and 4.4 and 12.6° in [{ZnBr$_2$(**1**)}$_6$], see Fig. S1 and S2† for atom labelling) leading to the bowed backbone seen in Fig. 1a. Twisting of the rings in the biphenyl unit is observed, consistent with relief of H···H repulsions between adjacent rings (angles between the rings containing N2/C16 and C19/C22 are 33.4 and 35.8° in [{ZnCl$_2$(**1**)}$_6$], and 34.2 and 36.9° in [{ZnBr$_2$(**1**)}$_6$]).

The packing of the hexacycles leads to the formation of a nanotube architecture with the tubes aligned parallel to the crystallographic c-axis (Fig. 2a). The tubes are filled with disordered solvent molecules and crystals are very sensitive to solvent loss, making structure determination difficult for the family of metallohexacycles reported in this work. The organization of molecules within each tube is best described by first considering the interdigitation of pendant phenyl rings of the biphenyl groups of every second metallohexacycle (Fig. 2b). Interlocking of two of the motifs shown in Fig. 2b results in the final nanotubular assembly shown in Fig. 2c. Between the hexacycles coloured red and blue in Fig. 2c, face-to-face π-stacking occurs between the pyridine ring containing atom N1 and the terminal phenyl ring with C22^{iii} (symmetry code iii = 1/3 + x, 2/3 + y, 5/3 + z); in [{ZnBr$_2$(**1**)}$_6$]·4CHCl$_3$·5MeOH·8H$_2$O,

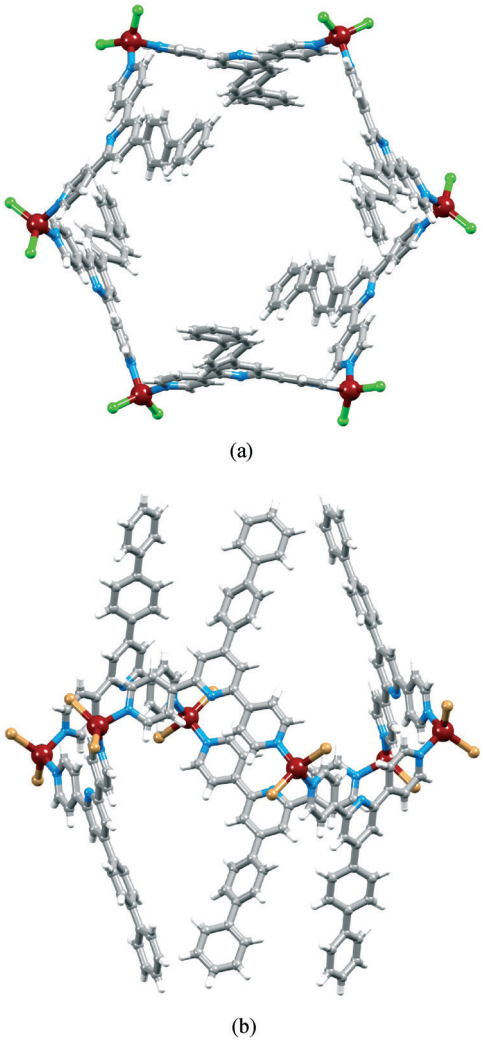

Fig. 1 Structures of (a) [{ZnCl$_2$(**1**)}$_6$] and (b) [{ZnBr$_2$(**1**)}$_6$] illustrating ring conformation **I**.

Table 1 Selected bond parameters in [{ZnCl$_2$(**1**)}$_6$]·6CHCl$_3$·6MeOH·5H$_2$O and [{ZnBr$_2$(**1**)}$_6$]·4CHCl$_3$·5MeOH·8H$_2$O. Symmetry codes: i = y, $-x + y$, $2 - z$; ii = y, $-x + y$, $-z$. See Fig. S1 and S2† for atom labelling

Bond distance/Å	[{ZnCl$_2$(**1**)}$_6$]	Bond distance/Å	[{ZnBr$_2$(**1**)}$_6$]
Zn1–N1	2.045(2)	Zn1–N1	2.0436(18)
Zn1–N3^{i}	2.050(3)	Zn1–N3^{ii}	2.0545(18)
Zn1–Cl1	2.2238(9)	Zn1–Br1	2.3612(4)
Zn1–Cl2	2.2051(8)	Zn1–Br2	2.3414(3)
Bond angle/°		**Bond angle/°**	
N1–Zn1–N3^{i}	103.77(11)	N1–Zn1–N3^{ii}	105.21(6)
N1–Zn1–Cl2	108.64(7)	N1–Zn1–Br2	107.80(5)
N3^{i}–Zn1–Cl2	106.12(7)	N3^{ii}–Zn1–Br2	106.78(5)
N1–Zn1–Cl1	104.11(7)	N1–Zn1–Br1	104.33(5)
N3^{i}–Zn1–Cl1	108.17(8)	N3^{ii}–Zn1–Br1	108.80(5)
Cl1–Zn1–Cl2	124.31(4)	Br1–Zn1–Br2	122.673(13)

the angle between the planes = 6.7° and distance between ring centroids = 3.77 Å and analogous parameters are 7.5° and 3.77 Å in the chlorido derivative. As Fig. 3a shows, each hexacycle is involved in six such interactions which contribute significantly

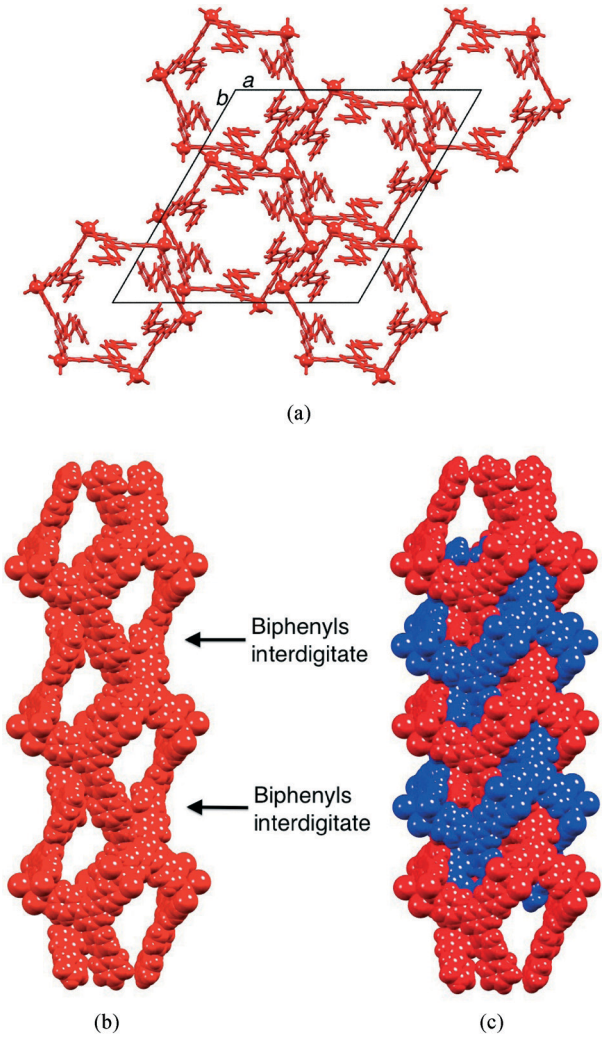

Fig. 2 (a) Hexacycles of $[\{ZnBr_2(\mathbf{1})\}_6]$ pack into tubes which follow the *c*-axis. (b) Within each tube, biphenyl domains of every second hexamer are interdigitated. (c) Interlocking of two of the motifs shown in (b). Solvent molecules are omitted.

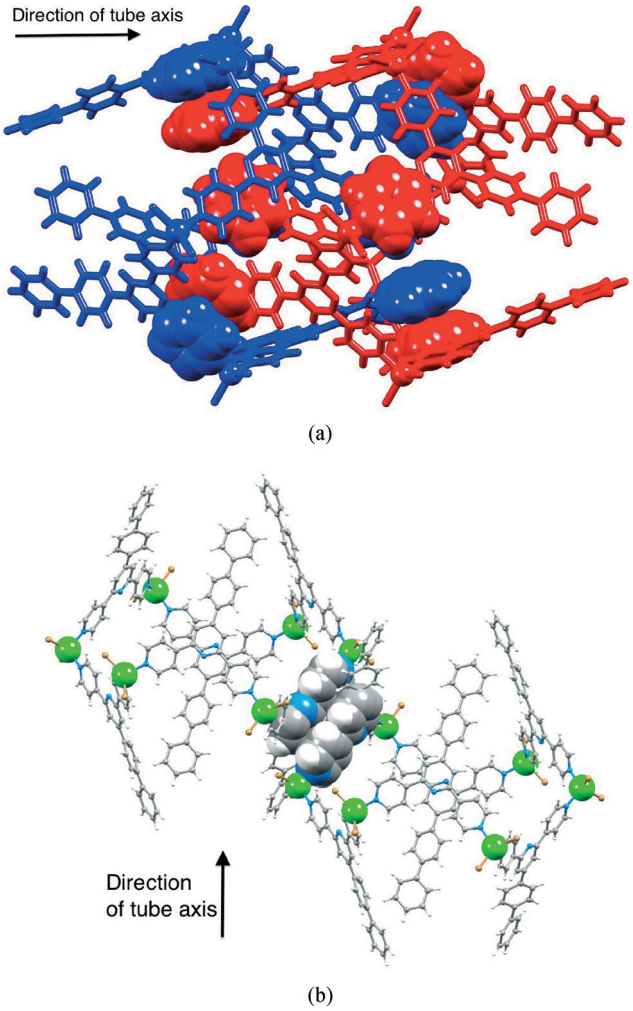

Fig. 3 (a) Face-to-face stacking of pyridine and phenyl rings between adjacent $[\{ZnBr_2(\mathbf{1})\}_6]$ molecules. (b) Face-to-face interaction between pairs of tpy units in adjacent tubes.

to the rigid architecture (see later). Adjacent tubes interact through π-stacking of 4,2′:6′,4″-tpy domains involving the rings containing N1/N2 and $N1^{iv}/N2^{iv}$ (symmetry code iv = 2/3 − *x*, 1/3 − *y*, −2/3 − *z*) (Fig. 3b). The angle between each pair of stacked pyridine rings is 4.4°, and the inter-centroid distance is 3.68 Å, making this an efficient interaction. Each hexamer is, by symmetry, involved in six such contacts.

The heavily disordered solvent molecules in the two structures have been modelled as partial occupancy H_2O, $CHCl_3$ and MeOH, with best models fitting formulations for the compounds of $[\{ZnCl_2(\mathbf{1})\}_6]\cdot 6CHCl_3\cdot 6MeOH\cdot 5H_2O$ and $[\{ZnBr_2(\mathbf{1})\}_6]\cdot 4CHCl_3\cdot 5MeOH\cdot 8H_2O$.

$[\{ZnCl_2(\mathbf{2})\}_6]$ and $[\{ZnBr_2(\mathbf{2})\}_6]$

Despite the fact that the replacement of hydrogen by fluorine in an organic compound can significantly affect solid-state structures,[30,31] we have observed that coordination polymers formed between zinc(II) acetate and ligands **1** and **2** are isostructural.[24] We were therefore intrigued to discover whether the same was true for the products of reactions between **1** and **2** with zinc(II) chloride or bromide. Ligand **2** was combined with $ZnCl_2$ or $ZnBr_2$ under the same room temperature conditions used for reactions with **1**. In contrast to the growth of only one type of crystal in reactions with **1**, treatment of **2** with either $ZnCl_2$ or $ZnBr_2$ resulted in the formation of colourless blocks and spear-like blocks, the latter being dominant in both reactions.

Structural analysis of the colourless blocks formed from $ZnCl_2$ and **2** confirmed the formation of discrete metallohexacycles in $[\{ZnCl_2(\mathbf{2})\}_6]\cdot 3CHCl_3\cdot 3MeOH\cdot 6H_2O$. The complex crystallizes in the trigonal space group $R\bar{3}$ with cell dimensions very similar to those in $[\{ZnCl_2(\mathbf{1})\}_6]\cdot 6CHCl_3\cdot 6MeOH\cdot 5H_2O$. The $[\{ZnCl_2(\mathbf{2})\}_6]$ hexacycle (Fig. 4a) contains tetrahedral zinc atoms (bond parameters are given in Table 2) and possesses the same conformation as in $[\{ZnCl_2(\mathbf{1})\}_6]$ with the pentafluorobiphenyl units in an alternating up/down arrangement around the ring (conformer **I**). Packing of the molecules into tube-like

assemblies running along the crystallographic *c*-axis mimics that in $[\{ZnCl_2(\mathbf{1})\}_6]\cdot 6CHCl_3\cdot 6MeOH\cdot 5H_2O$, with disordered solvent molecules (modelled with partial occupancies) filling the tubes. Packing of $[\{ZnCl_2(\mathbf{2})\}_6]$ hexacycles can be described in the same manner as for $[\{ZnCl_2(\mathbf{1})\}_6]$, but with pentafluorophenyl–pyridine ($\pi_F\cdots\pi_H$) face-to-face π-stacking replacing phenyl–pyridine π-contacts (compare Fig. 4b with Fig. 3a). For the $\pi_F\cdots\pi_H$ interaction in $[\{ZnCl_2(\mathbf{2})\}_6]$, the angle between the planes is 7.8° and the distance between ring centroids is 3.71 Å. Packing of tubes involves analogous tpy–tpy face-to-face interactions as detailed for $[\{ZnBr_2(\mathbf{1})\}_6]$ (Fig. 3b); stacked rings lie at 2.2° to one another and the inter-centroid separation is 3.58 Å.

A combination of rapid solvent loss from the block-like crystals formed in the reaction of $ZnBr_2$ and **2**, and heavily disordered solvent, meant that the program SQUEEZE[29] was used to treat the data. Structure determination confirmed the presence of $[\{ZnBr_2(\mathbf{2})\}_6]$ hexacycles. The trigonal space group and cell dimensions were consistent with those determined for all three structures described above, and Fig. 5 shows that the ring adopts conformer **I** mimicking that in $[\{ZnCl_2(\mathbf{1})\}_6]$, $[\{ZnBr_2(\mathbf{1})\}_6]$ (Fig. 1b) and $[\{ZnCl_2(\mathbf{2})\}_6]$.

The spear-like blocks from the reactions of $ZnCl_2$ or $ZnBr_2$ and **2** proved to be a second conformer (conformer **II**) of the metallohexacycle. The X-ray crystal structure of the chlorido complex $[\{ZnCl_2(\mathbf{2})\}_6]$ confirmed the presence of a chair conformer that replicates that observed in $[\{ZnCl_2(\mathbf{4})\}_6]$ (**4** = 4′-(4-ethynylphenyl)-4,2′:6′,4″-terpyridine).[19] Excessive solvent disorder in the large void space was handled using the program SQUEEZE.[29] $[\{ZnCl_2(\mathbf{2})\}_6]$ crystallizes in the monoclinic space group $P2_1/n$, with half of the metallomacrocycle in the asymmetric unit; the second half is generated through an inversion centre. Each Zn atom is tetrahedrally coordinated with Zn–N bond distances in the range 2.026(2) to 2.070(2) Å and Zn–Cl bond lengths ranging from 2.2157(8) to 2.2519(10) Å. Fig. 6 shows two views of the structure of $[\{ZnCl_2(\mathbf{2})\}_6]$, and a comparison with Fig. 1 highlights the differences between conformations **I** and **II**. One pentafluorobiphenyl unit in conformer **II** of $[\{ZnCl_2(\mathbf{2})\}_6]$ is disordered and has been modelled over two positions of fractional occupancies 0.79 and 0.21; only one site is shown in Fig. 6. The chair-conformers pack into columns which run parallel to the *a*-axis (Fig. 7a), with

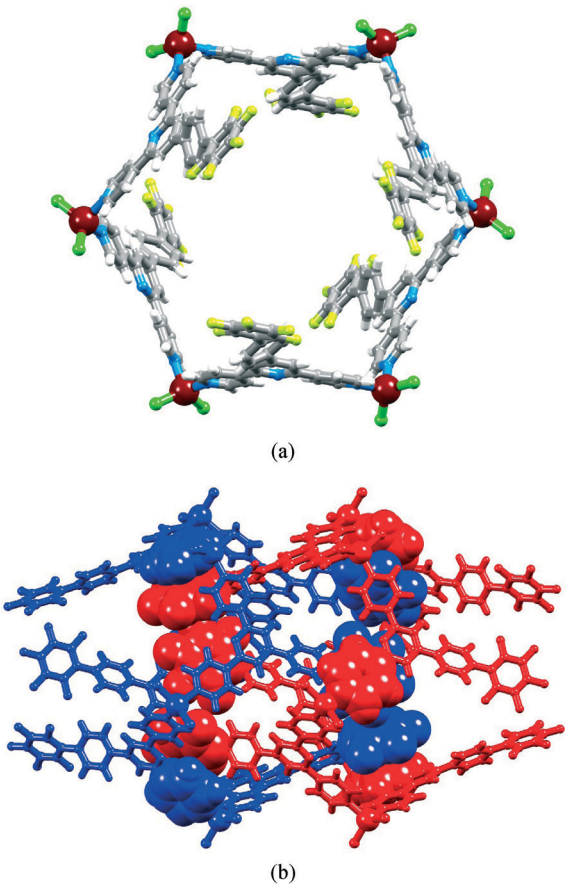

Fig. 4 (a) Structure of the $[\{ZnCl_2(\mathbf{2})\}_6]$ hexamer in $[\{ZnCl_2(\mathbf{2})\}_6]\cdot 3CHCl_3\cdot 3MeOH\cdot 6H_2O$. (b) Face-to-face stacking of pyridine and pentafluorophenyl rings between adjacent $[\{ZnCl_2(\mathbf{2})\}_6]$ hexamers.

Table 2 Selected bond parameters in $[\{ZnCl_2(\mathbf{2})\}_6]\cdot 3CHCl_3\cdot 3MeOH\cdot 6H_2O$ and $[\{ZnBr_2(\mathbf{2})\}_6]$. Symmetry codes: i = $x - y + 2/3$, $x + 1/3$, $1/3 - z$. See Fig. S3 and S4† for atom labelling

Bond distance/Å	$[\{ZnCl_2(\mathbf{1})\}_6]$	Bond distance/Å	$[\{ZnBr_2(\mathbf{1})\}_6]$
Zn1–N1^i	2.0510(19)	Zn1–N1^i	2.068(4)
Zn1–N3	2.0522(18)	Zn1–N3	2.039(4)
Zn1–Cl1	2.2126(7)	Zn1–Br1	2.3454(8)
Zn1–Cl2	2.2212(8)	Zn1–Br2	2.3541(9)
Bond angle/°		**Bond angle/°**	
N1^i–Zn1–N3	106.26(8)	N1^i–Zn1–N3	107.51(17)
N1^i–Zn1–Cl2	103.19(6)	N1^i–Zn1–Br2	103.34(11)
N3–Zn1–Cl2	108.24(6)	N3–Zn1–Br2	108.27(13)
N1^i–Zn1–Cl1	105.33(5)	N1^i–Zn1–Br1	105.19(10)
N3–Zn1–Cl1	104.74(6)	N3–Zn1–Br1	105.42(11)
Cl1–Zn1–Cl2	127.49(3)	Br1–Zn1–Br2	125.98(3)

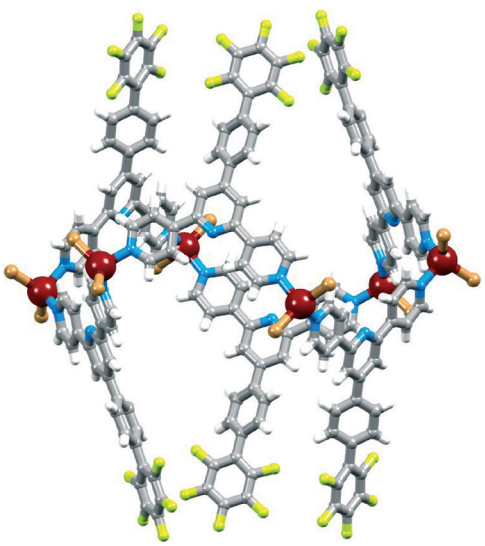

Fig. 5 Structure of hexamer $[\{ZnBr_2(\mathbf{2})\}_6]$ showing the alternating up/down arrangement of the pentafluorophenyl units (conformer **I**).

protruding pentafluorophenyl units of one column interdigitated with those of an adjacent column. However, the interdigitation involves pyridine–phenyl $\pi_H\cdots\pi_H$ contacts and does not involve the pentafluorophenyl domains. Intermolecular $\pi_F\cdots\pi_H$(pyridine) interactions operate between adjacent $[\{ZnCl_2(\mathbf{2})\}_6]$ molecules within a column (Fig. 7a), but only involve one of the three independent 4,2′:6′,4″-tpy ligands (that containing N8 and F13, see Fig. S5† for labelling). The angle between the planes through the rings containing N8 and F13^{i} (symmetry code i = −1 + *x*, *y*, *z*) is 5.0° and the distance between ring centroids = 3.96 Å. Each hexacycle participates in four such stacking interactions.

Preliminary data only were obtained for the spear-like blocks obtained from reaction of $ZnBr_2$ and **2**. Crystals of this habit were repeatedly obtained as the major product in a number of crystallization attempts, but were always of poor quality. Solvent loss was a persistent problem. The preliminary structure determination established the presence of the chair-like conformer of $[\{ZnBr_2(\mathbf{2})\}_6]$, thus confirming that $[\{ZnBr_2(\mathbf{2})\}_6]$, like $[\{ZnCl_2(\mathbf{2})\}_6]$, crystallizes with conformers **I** and **II**. Although both conformers pack into tube-like assemblies, the intermolecular interactions between molecules of conformer **I**, both within a tube and between adjacent tubes, generate a more rigid architecture than those of conformer **II**. The void spaces (calculated using PLATON[29]) in the lattices

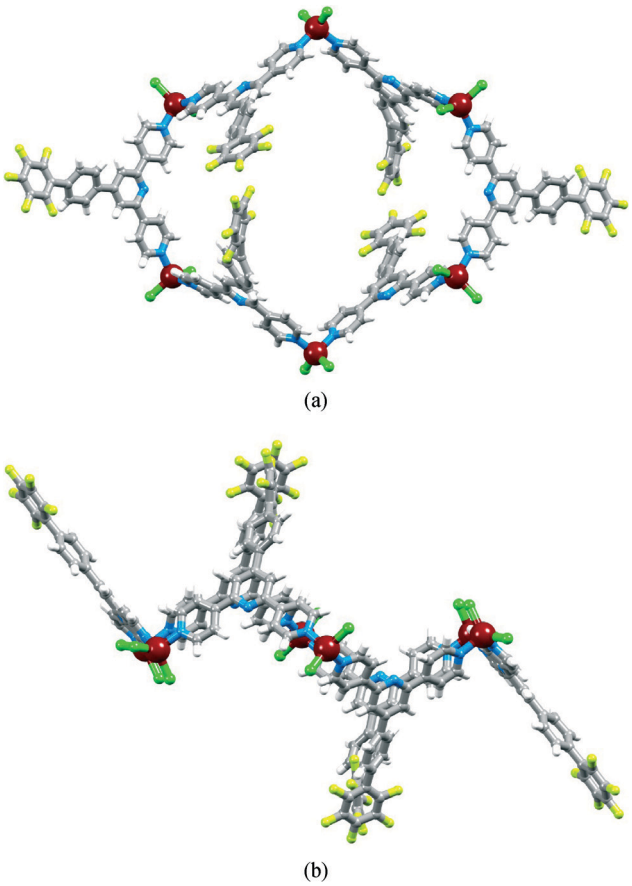

Fig. 6 Structure of conformer **II** of $[\{ZnCl_2(\mathbf{2})\}_6]$ (a) viewed through the macrocycle and (b) showing the chair conformation.

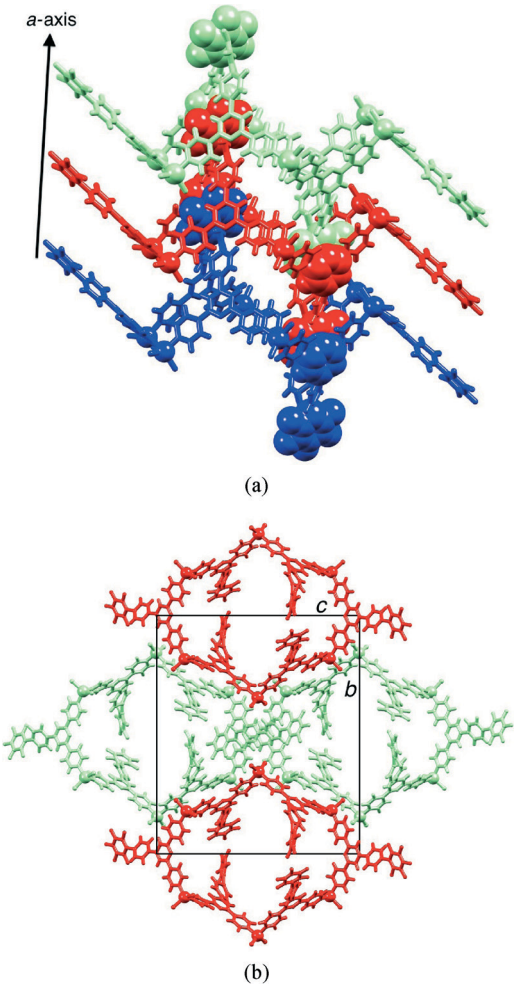

Fig. 7 Packing of molecules of $[\{ZnCl_2(\mathbf{2})\}_6]$ with conformer **II**: (a) part of one column showing $\pi_F\cdots\pi_H$(pyridine) contacts, and (b) view down the *a*-axis showing four adjacent columns.

of the two conformers of $[\{ZnCl_2(\mathbf{2})\}_6]$ are 26.8% for conformer **I** and 27.6% for conformer **II**, while for $[\{ZnBr_2(\mathbf{2})\}_6]$, the corresponding values are 28.3 and 33.1%.

Interestingly, crystallization by layering a chloroform solution of $ZnCl_2$ with a 1 : 1 mixture of ligands **1** and **2** in methanol resulted in a compound which crystallizes in the trigonal space group $R\bar{3}$ with cell dimensions (ESI†) essentially the same as those of $[\{ZnCl_2(\mathbf{1})\}_6]\cdot 6CHCl_3\cdot 6MeOH\cdot 5H_2O$ and $[\{ZnCl_2(\mathbf{2})\}_6]\cdot 3CHCl_3\cdot 3MeOH\cdot 6H_2O$. Single crystal X-ray analysis confirmed the assembly of $[\{ZnCl_2(\mathbf{L})\}_6]$ in conformation **I**, with **1** and **2** statistically disordered over one ligand site. We have observed a similar disorder phenomenon in the coordination polymer $[Cu_2(\mu\text{-}OAc)_4(\mathbf{1})]_n\cdot[Cu_2(\mu\text{-}OAc)_4(\mathbf{2})]_n$.[24]

From phenyl to naphthyl: $[\{ZnBr_2(\mathbf{3})\}_6]$

In principle, interconversion of conformers **I** and **II** of $[\{ZnX_2(L)\}_6]$ (L = **1** or **2**, X = Cl or Br) may occur through rotation around the Zn–N bonds. The arrangement of the biphenyl or pentafluorobiphenyl units in conformer **I** appears to

be ideal to host arene guests of appropriate dimensions (*e.g.* fullerenes), and we argued that a preference for conformer **I** might be dictated by interactions with suitable guest molecules. Host–guest interactions should be further enhanced by replacing the terminal phenyl or pentafluorophenyl rings in **1** and **2** by more extended aromatic systems, and we chose the naphthyl domain for initial studies (ligand **3**, Scheme 2).

The formation of hexamer $[\{ZnBr_2(\mathbf{3})\}_6]$ was established by single crystal X-ray analysis of colourless blocks of $[\{ZnBr_2(\mathbf{3})\}_6]\cdot 3CHCl_3\cdot 15H_2O$ that grew from the reaction of $ZnBr_2$ with **3**. Crystallization in the trigonal space group $R\bar{3}$ is consistent with the presence of conformer **I**, and the contents of the asymmetric unit and atom labelling are given in Fig. S6.† Fig. 8 shows the structure of the metallohexacycle. The bond lengths within the tetrahedral coordination sphere of Zn1 are Zn1–N1 = 2.064(2), Zn1–N3^{i} = 2.049(2), Zn1–Br1 = 2.3581(4), Zn1–Br2 = 2.3599(4) Å (symmetry code i = −1/3 + *y*, 1/3 − *x* + *y*, 4/3 − *z*) with bond angles of N3^{i}–Zn1–N1 = 111.28(8) and Br1–Zn1–Br2 = 124.127(18)° and N–Zn1–Br angles in the range 104.02(6) to 108.26(6)°. The naphthalen-1-ylphenyl unit is disordered and has been modelled over two sites (related by a wagging motion) of occupancies 0.41 and 0.59. The slight bowing of the tpy backbone (angles between the planes of adjacent pyridine rings = 9.7 and 3.3°) and the twisting of the phenyl ring with respect to pyridine and naphthyl units to which it is bonded (interplane angles = 40.8 and 44.3°) are consistent with the related structures described above. $[\{ZnBr_2(\mathbf{3})\}_6]$ hexamers stack into tubes along the *c*-axis in an analogous manner to that detailed in Fig. 2 and the accompanying discussion. Interdigitation of naphthalen-1-ylphenyl units occurs between every second $[\{ZnBr_2(\mathbf{3})\}_6]$ molecule, and adjacent metallohexacycles engage in face-to-face π-stacking of naphthyl and pyridine rings (Fig. 9). The angle between the least squares planes through the pyridine ring containing N3 and the naphthyl unit is 7.3°, and the distances from the centroid of the pyridine ring to those of the rings comprising the naphthyl unit are 3.67 and 4.00 Å. The closest separation of any pair of naphthyl units on one rim of the $[\{ZnBr_2(\mathbf{3})\}_6]$ hexacycle is ≈11 Å (C29···C29^{ii} = 11.1 Å, symmetry code ii = −*x* + *y*, 1 − *x*, *z*, see Fig. S6† for atom labels) and this compares to the diameter of a C_{60} molecule of ≈7 Å (10 Å van der Waals diameter). Thus, the cavity is suited to acting as a host for the fullerene.

Preliminary data from structural analysis of crystals grown from reactions of $ZnCl_2$ and ligand **3** confirmed the assembly of the anticipated hexamer $[\{ZnCl_2(\mathbf{3})\}_6]$ with conformation **I** as described for the analogous bromido complex. However, the naphthyl units were heavily disordered, and this was a persistent problem despite modifying the crystallization conditions.

Fullerene encapsulation: $[2\{ZnCl_2(\mathbf{3})\}_6\cdot C_{60}]\cdot 6MeOH\cdot 16H_2O$

Porphyrin and calixarene[32,33] (in particular calix[5]arene)[34] derivatives are popular choices as hosts for C_{60}, with the fullerene typically occupying the bowl-shaped cavity of the host. An example of a dumb-bell shaped metallo-bis(calixarene) (in which two tetrathiacalix[4]arenes are connected through coordination to manganese(II) centres) breaks this pattern with the C_{60} guests interacting with the concave outer surface of the dumb-bell in preference to occupying the calixarene cavities.[35] In contrast, both the inner and outer faces of a porphyrin barrel (a tetrameric metalloporphyrin complex) interact with C_{60}, giving rise to a 1:3 host:guest compound in the solid state.[36] Examples of metallomacrocycles hosting C_{60} appear to be limited. Maverick and coworkers have described C_{60} encapsulation by a molecular square comprising ditopic β-ketonate ligands bound to square planar copper(II) ions.[37] Several examples of cyclic metallo-bisporphyrins binding fullerene guests have been reported.[38–42] Of particular relevance to the results reported below is the use of pyridyl-decorated bis(nickellaporphyrin) domains which assemble into one-dimensional tubes in the solid state by virtue of

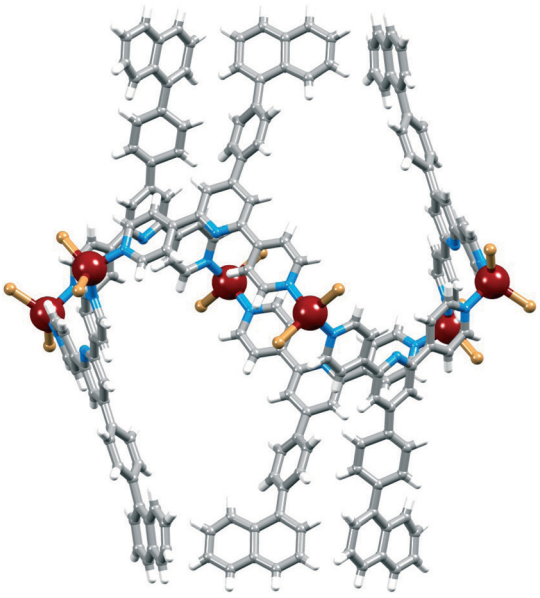

Fig. 8 Structure of the centrosymmetric $[\{ZnBr_2(\mathbf{3})\}_6]$ molecule in $[\{ZnBr_2(\mathbf{3})\}_6]\cdot 3CHCl_3\cdot 15H_2O$; the metallohexacycle adopts conformer **I**.

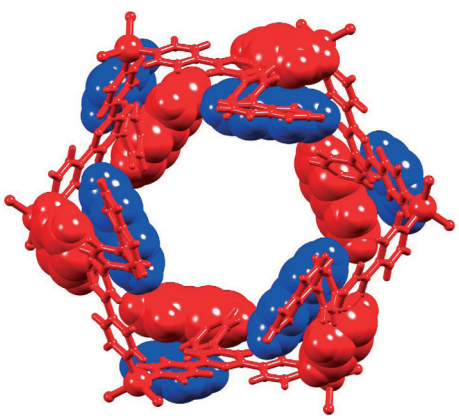

Fig. 9 View down the *c*-axis in $[\{ZnBr_2(\mathbf{3})\}_6]\cdot 3CHCl_3\cdot 15H_2O$ (solvents omitted) showing face-to-face π-stacking of naphthyl and pyridine domains between adjacent hexamers.

pyridine···pyridine face-to-face π-interactions augmented by CH···$N_{pyrrole}$ contacts.[41,42]

We considered two approaches for the formation of host–guest complexes using $[\{ZnX_2(L)\}_6]$ metallomacrocycles as hosts. The first strategy of trapping guest molecules within pre-formed hosts relies upon the retention of the metallohexacycles in solution. Unfortunately, we have no unambiguous evidence that the $[\{ZnX_2(L)\}_6]$ complexes remain intact in solution. Attempts to obtain ESI mass spectra were unsuccessful; the MALDI TOF mass spectrum of $[\{ZnCl_2(\mathbf{1})\}_6]$ showed a base (and dominant) peak at *m*/*z* 869.5 which was assigned to the fragment $[Zn(\mathbf{1})_2Cl]^+$ (calc. *m*/*z* 869.2). The electronic absorption spectrum of a solution made by dissolving crystalline $[\{ZnCl_2(\mathbf{1})\}_6]$ in MeOH (1×10^{-5} mol dm^{-3}) was identical to that of the free ligand,[23] suggesting dissociation of the complex. The aromatic region of the ^{1}H NMR spectrum of a CD_3OD solution of $[\{ZnCl_2(\mathbf{3})\}_6]$ matched that of the free ligand **3** in the same solvent. A similar result was obtained for a $CDCl_3$ solution.

The second strategy for the formation of the host–guest complex involves the assembly of the $[\{ZnX_2(L)\}_6]$ host from ZnX_2 and L in the presence of the guest species. Single crystals suitable for X-ray diffraction were obtained within 2 weeks by carefully layering 1,2-$Cl_2C_6H_4$–MeOH solutions of **3**, C_{60} and $ZnCl_2$ at room temperature. A ratio of $ZnCl_2$: **3** : C_{60} = 6 : 6 : 1 was chosen in anticipation of encapsulation of one C_{60} molecule per metallohexacycle. Subsequent experiments with different amounts of C_{60} resulted in crystals with the same structure as that described below and of crystals of excess C_{60}. The product was confirmed to be $[2\{ZnCl_2(\mathbf{3})\}_6{\cdot}C_{60}]{\cdot}6MeOH{\cdot}16H_2O$ and crystallized in the trigonal space group $R\bar{3}$, with a unit cell having a *c*-axis approximately double the length of those found for the hexamers with conformer **I** described above, and with two independent $\{ZnCl_2(\mathbf{3})\}$ units and one-sixth of a fullerene molecule in the asymmetric unit. Two mutually stacked hexamers and one C_{60} molecule (Fig. 10a) are generated using 3-fold rotoinversion. The general architectures of the two independent $[\{ZnCl_2(\mathbf{3})\}_6]$ molecules in $[2\{ZnCl_2(\mathbf{3})\}_6{\cdot}C_{60}]{\cdot}6MeOH{\cdot}16H_2O$ are similar and do not differ significantly from those of free $[\{ZnCl_2(\mathbf{3})\}_6]$ and $[\{ZnBr_2(\mathbf{3})\}_6]$. However, it is significant that in $[2\{ZnCl_2(\mathbf{3})\}_6{\cdot}C_{60}]$, the $\{ZnCl_2(\mathbf{3})\}_6$ hexamer that associates most closely with C_{60} contains an ordered naphthyl group, while in the second, the naphthyl unit is disordered and has been modelled over two positions with site occupancies 0.67 and 0.33. In the discussion below, we consider only the major occupancy site. The twist angles between the bonded phenyl–pyridine rings are 37.8 and 33.2° in the molecules coloured green and yellow in Fig. 10a compared to 40.8° in $[\{ZnBr_2(\mathbf{3})\}_6]$. The angles between the planes through the phenyl and naphthyl units in the molecules coloured green and yellow in Fig. 10a are 43.8 and 46.3°, respectively, compared to 44.3° in $[\{ZnBr_2(\mathbf{3})\}_6]$. Just as in $[\{ZnBr_2(\mathbf{3})\}_6]$, the structure of $[2\{ZnCl_2(\mathbf{3})\}_6{\cdot}C_{60}]{\cdot}6MeOH{\cdot}16H_2O$ is best described in terms of the interdigitation of naphthalen-1-ylphenyl units between every second $[\{ZnCl_2(\mathbf{3})\}_6]$ molecule, coupled with an interlocking of two sets of these assemblies (compare Fig. 10 with Fig. 2). Fig. 10b shows two non-adjacent $[\{ZnCl_2(\mathbf{3})\}_6]$ hexamers and highlights the interdigitated naphthalen-1-ylphenyl units. Adjacent metallohexacycles (yellow and green in Fig. 10) participate in face-to-face π-stacking of naphthyl and pyridine rings. Each C_{60} molecule is captured between six naphthyl units, three from one $[\{ZnCl_2(\mathbf{3})\}_6]$ hexamer, and three from its interdigitated partner (centre of Fig. 10b). Further, the fullerene–six-naphthyl (green in Fig. 10) assembly lies at the heart of the second (yellow in Fig. 10) $[\{ZnCl_2(\mathbf{3})\}_6]$ hexamer. The C_{60} molecule is crystallographically ordered, presumably a consequence of its π-stacking interactions with the naphthyl groups of the host. The closest separations of the centroid of the C_6-ring of the fullerene

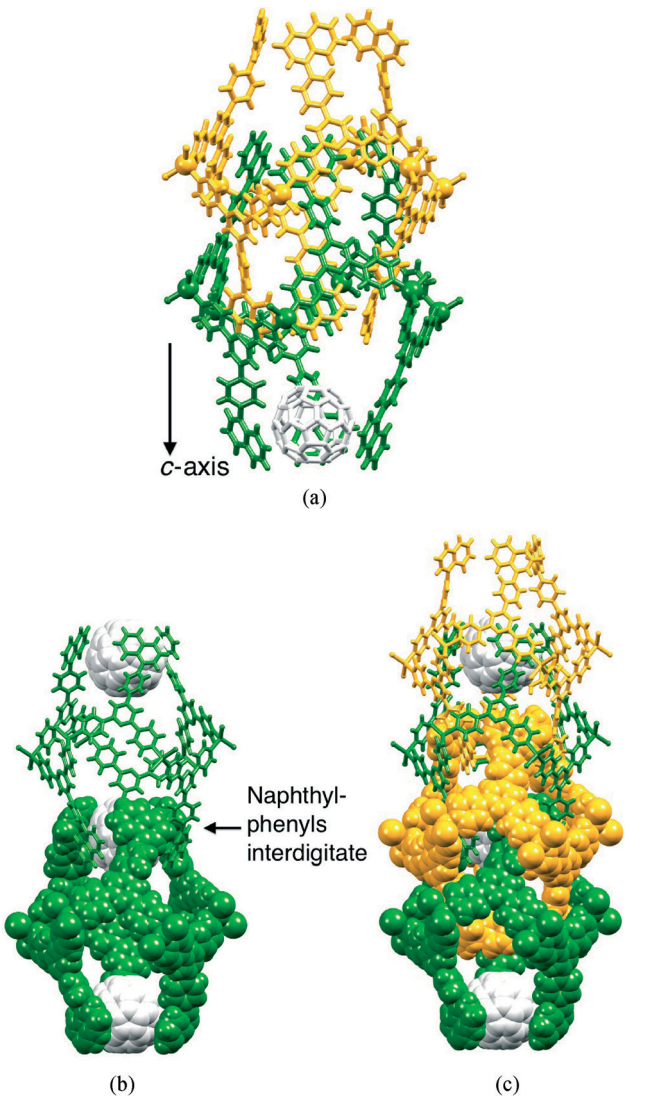

Fig. 10 (a) The two independent $[\{ZnCl_2(\mathbf{3})\}_6]$ hexamers and one C_{60} molecule present in $[2\{ZnCl_2(\mathbf{3})\}_6{\cdot}C_{60}]{\cdot}6MeOH{\cdot}16H_2O$. Only the major occupancy sites of the disordered naphthyl groups (yellow) are shown. (b) Interdigitated naphthalen-1-ylphenyl units of every second hexamer (coloured green) host a C_{60} molecule. (c) Interlocking of the crystallographically independent $[\{ZnCl_2(\mathbf{3})\}_6]$ hexamers (coloured green and yellow) completes the structure. Solvent molecules are omitted.

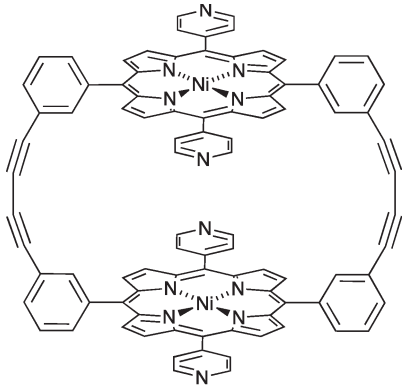

5

Scheme 3 Structure of the bis(nickellaporphyrin) complex **5** reported by Tani and coworkers.[41,42]

to centroids of the two rings making up the naphthyl group are 3.78 and 4.08 Å. It is noteworthy that only every other set of interdigitated naphthyl units (green in Fig. 10) hosts a fullerene. The cavity between the naphthyl units of the [{$ZnCl_2$(**3**)}$_6$] hexamers coloured yellow in Fig. 10 is dimensionally similar to that between the hexamers coloured green, but is filled with disordered solvent. The latter have been modelled as partial occupancy H_2O and MeOH molecules.

Our attempts to introduce further fullerene into the host (see above) were not successful, begging the question as to why only every other cavity is occupied. The spatial properties of each centrosymmetric cavity are essentially the same, and the distance between the middles of empty (yellow in Fig. 10c) and occupied (green) cavities is 11.27 Å. The corresponding separation in crystalline C_{60} or co-crystallized C_{60}·Z where Z is a small organic molecule, is close to 10 Å,[43–46] indicating that steric crowding is not the origin of the half-filling of cavities by ordered C_{60} in [2{$ZnCl_2$(**3**)}$_6$·C_{60}]·6MeOH·16H_2O. We propose that the observed structure and periodic occupancies of cavities by the fullerene are a consequence of the assembly process, and that capture of C_{60} by a three-naphthyl domain of one hexacycle is probably an early recognition event. A search of the CSD[21] (v. 5.34 with November 2012 updates using Conquest v. 1.15[22]) indicates that the structure of [2{$ZnCl_2$(**3**)}$_6$·C_{60}]·6MeOH·16H_2O is unusual. The intimate interlocking of [{$ZnCl_2$(**3**)}$_6$] hexamers along a tube appears to be a critical feature that prevents the C_{60} molecules from occupying every six-naphthyl host. A relevant example for comparison is metallocycle **5** (Scheme 3). In the solid state, these molecules form one-dimensional tubes, supported by intermolecular pyridine···pyridine π-stacking interactions and CH···$N_{pyrrole}$ contacts. The tube-like assembly is more open than that formed by the [{$ZnCl_2$(**3**)}$_6$] hexamers and **5** forms a 1 : 1 host–guest complex with C_{60}, *i.e.* every macrocyclic cavity hosts a C_{60} molecule.[41,42] Other metallomacrocyclic hosts crystallize with C_{60} in 1 : 1 assemblies, but there is no interlocking of the metallomacrocycles to form tubes.[37–40]

Conclusions

The formation of metallohexacycles has been shown to be a persistent phenomenon in the reactions of the 4′-aryl-substituted 4,2′:6′,4″-terpyridines **1**, **2** or **3** with $ZnCl_2$ or $ZnBr_2$. Whereas [{$ZnCl_2$(**1**)}$_6$] and [{$ZnBr_2$(**1**)}$_6$] adopt a conformation (conformer **I**) in which the biphenyl domains are in an alternating up/down arrangement, both the tub-like conformer **I** and chair-like conformer **II** (dominant form) are observed when the pentafluorophenyl domain is present in [{$ZnCl_2$(**2**)}$_6$] and [{$ZnBr_2$(**2**)}$_6$]. Both conformers stack into tubes in the solid-state, the architecture formed by conformer **I** being more rigid than that assembled from conformer **II**. This leads to more robust crystals for conformer **I**. Hexamers of conformer **I** pack into tubes. Within each tube, biphenyl domains of every second hexamer are interdigitated, producing motifs which engage in pyridine–phenyl face-to-face contacts forming an interlocked, rigid nanotube. π-Stacking between 4,2′:6′,4″-tpy domains operates between adjacent tubes.

The naphthalen-1-ylphenyl-containing ligand **3** reacts with $ZnCl_2$ or $ZnBr_2$ to give hexameric [{$ZnCl_2$(**3**)}$_6$] or [{$ZnBr_2$(**3**)}$_6$] exhibiting conformer **I**. If the reaction is carried out in the presence of C_{60}, crystals of [2{$ZnCl_2$(**3**)}$_6$·C_{60}]·6MeOH·16H_2O are isolated. This contains hexacyclic [{$ZnCl_2$(**3**)}$_6$] molecules in conformer **I**, replicating the structure of the parent host and its analogue [{$ZnBr_2$(**3**)}$_6$]. The host–guest complex comprises a tube-like structure that mimics that found in [{$ZnCl_2$(**3**)}$_6$] and [{$ZnBr_2$(**3**)}$_6$], and in analogous complexes containing [{ZnX_2(**1**)}$_6$] and [{ZnX_2(**2**)}$_6$] in conformer **I**. Each crystallographically-ordered C_{60} is trapped between six ordered naphthyl units, three from one hexamer and three from its interdigitated partner, and the C_{60}–six-naphthyl unit sits at the centre of a second [{$ZnCl_2$(**3**)}$_6$] macrocycle. The structure is highly unusual in having an ordered array of C_{60} guests occupying every other available cavity in a tube. All spatial properties of all the six-naphthyl cavities in the lattice are essentially the same, and the distance between them is greater than the separation of C_{60} molecules in crystalline C_{60} and related structures. Thus, on steric grounds, the 'empty' cavity could, in principle, host a fullerene. Thus, we suggest that the observed structure and periodic occupancies of cavities by the fullerene are intimately associated with the assembly process.

Acknowledgements

We thank the Swiss National Science Foundation, the European Research Council (advanced grant 267816 LiLo) and the University of Basel for financial support. We are grateful to Dr. Markus Neuburger for thought-provoking discussions.

Notes and references

1 G. F. Swiegers and T. J. Malefetse, *Chem.–Eur. J.*, 2001, **7**, 3636.

2 G. F. Swiegers and T. J. Malefetse, *Coord. Chem. Rev.*, 2002, **225**, 91.
3 B. H. Northrop, Y.-R. Zheng, K.-W. Chi and P. J. Stang, *Acc. Chem. Res.*, 2009, **42**, 1554.
4 E. C. Constable and C. E. Housecroft, in *Comprehensive Inorganic Chemistry II*, ed. J. Reedijk and K. R. Poeppelmeier, Elsevier, Oxford, 2013, vol. 8, ch. 8.23, pp. 1–29.
5 See for example: P. J. Stang, D. H. Cao, S. Saito and A. M. Arif, *J. Am. Chem. Soc.*, 1995, **117**, 6273.
6 See for example: G. R. Newkome, T. J. Cho, C. N. Moorefield, R. Cush, P. S. Russo, L. A. Godínez, M. J. Saunders and P. Mohapatra, *Chem.–Eur. J.*, 2002, **8**, 2946.
7 G. F. Swiegers and T. J. Malefeste, *Chem. Rev.*, 2000, **100**, 3483.
8 M. Köberl, M. Cokoja, W. A. Herrmann and F. E. Kühn, *Dalton Trans.*, 2011, **40**, 6834.
9 S. Bureekaew, S. Amirjalayer and R. Schmid, *J. Mater. Chem.*, 2012, **22**, 10249.
10 S. I. Vagin, A. K. Ott and B. Rieger, *Chem. Ing. Tech.*, 2007, **79**, 767.
11 D. J. Tranchemontagne, J. L. Mendoza-Corés, M. O'Keeffe and O. M. Yaghi, *Chem. Soc. Rev.*, 2009, **38**, 1257.
12 M. Eddaoudi, D. B. Moler, H. Li, B. Chen, T. M. Reineke, M. O'Keeffe and O. M. Yaghi, *Acc. Chem. Res.*, 2001, **34**, 319.
13 M. Barquin, J. Cancela, M. J. González Garmendia, J. Quintanilla and U. Amador, *Polyhedron*, 1998, **17**, 2373.
14 B.-C. Wang, Q.-R. Wu, H.-M. Hu, X.-L. Chen, Z.-H. Yang, Y.-Q. Shangguan, M.-L. Yang and G.-L. Xue, *CrystEngComm*, 2010, **12**, 485.
15 X.-Z. Li, M. Li, Z. Li, J.-Z. Hou, X.-C. Huang and D. Li, *Angew. Chem., Int. Ed.*, 2008, **47**, 6371.
16 L. Hou and D. Li, *Inorg. Chem. Commun.*, 2005, **8**, 190.
17 G. W. V. Cave and C. L. Raston, *J. Supramol. Chem.*, 2002, **2**, 317.
18 E. C. Constable, C. E. Housecroft, P. Kopecky, M. Neuburger, J. A. Zampese and G. Zhang, *CrystEngComm*, 2012, **14**, 446.
19 E. C. Constable, G. Zhang, C. E. Housecroft and J. A. Zampese, *CrystEngComm*, 2011, **13**, 6864.
20 J. Heine, J. Schmedt auf der Günne and S. Dehnen, *J. Am. Chem. Soc.*, 2011, **133**, 10018.
21 F. H. Allen, *Acta Crystallogr., Sect. B: Struct. Sci.*, 2002, **58**, 380.
22 I. J. Bruno, J. C. Cole, P. R. Edgington, M. K. Kessler, C. F. Macrae, P. McCabe, J. Pearson and R. Taylor, *Acta Crystallogr., Sect. B: Struct. Sci.*, 2002, **58**, 389.
23 E. C. Constable, C. E. Housecroft, M. Neuburger, J. Schönle, S. Vujovic and J. A. Zampese, *Polyhedron*, 2013, **60**, 120.
24 E. C. Constable, C. E. Housecroft, S. Vujovic, J. A. Zampese, A. Crochet and S. R. Batten, *CrystEngComm*, 2013, **15**, 10068, in press.
25 E. C. Constable, C. E. Housecroft, J. Schönle, S. Vujovic and J. A. Zampese, *Polyhedron*, 2013, **60**, 120.
26 Bruker Analytical X-ray Systems, Inc., 2006, *APEX2, version 2 User Manual, M86-E01078*, Madison, WI.
27 G. M. Sheldrick, *Acta Crystallogr., Sect. A: Found. Crystallogr.*, 2008, **64**, 112.
28 C. F. Macrae, I. J. Bruno, J. A. Chisholm, P. R. Edgington, P. McCabe, E. Pidcock, L. Rodriguez-Monge, R. Taylor, J. van de Streek and P. A. Wood, *J. Appl. Crystallogr.*, 2008, **41**, 466.
29 A. L. Spek, *Acta Crystallogr., Sect. D: Biol. Crystallogr.*, 2009, **65**, 148.
30 K. Reichenbächer, H. I. Süss and J. Hulliger, *Chem. Soc. Rev.*, 2005, **34**, 22.
31 R. Berger, G. Resnati, P. Metrangolo, E. Weber and J. Hulliger, *Chem. Soc. Rev.*, 2011, **40**, 3496.
32 K. Tashiro and T. Aida, *Chem. Soc. Rev.*, 2007, **36**, 189.
33 D. Canevet, E. M. Pérez and N. Martín, *Angew. Chem., Int. Ed.*, 2011, **50**, 9248.
34 See for example: T. Haino, M. Yanase and Y. Fukazawa, *Tetrahedron Lett.*, 1997, **38**, 3739; J. L. Atwood, L. J. Barbour, P. J. Nichols, C. L. Raston and C. A. Sandoval, *Chem.–Eur. J.*, 1999, **5**, 990; J. L. Atwoood, L. J. Barbour, M. W. Heaven and C. L. Raston, *Angew. Chem., Int. Ed.*, 2003, **42**, 3254; M. Makha, M. J. Hardie and C. L. Raston, *Chem. Commun.*, 2002, 1446.
35 Y. Bi, W. Liao, X. Wang, X. Wang and H. Zhang, *Dalton Trans.*, 2011, **40**, 1849.
36 J. Song, N. Aratani, H. Shinokubo and A. Osuka, *J. Am. Chem. Soc.*, 2010, **132**, 16356.
37 C. Pariya, C. R. Sparrow, C.-K. Back, G. Sandí, F. R. Fronczek and A. W. Maverick, *Angew. Chem., Int. Ed.*, 2007, **46**, 6305.
38 J.-Y. Zheng, K. Tashiro, Y. Hirabayashi, K. Kinbara, K. Saigo, T. Aida, S. Sakamoto and K. Yamaguchi, *Angew. Chem., Int. Ed.*, 2001, **40**, 1858.
39 M. Yanagisawa, K. Tashiro, M. Yamasaki and T. Aida, *J. Am. Chem. Soc.*, 2007, **129**, 11912.
40 L. P. Hernández-Eguía, E. C. Escudero-Adán, I. C. Pintre, B. Ventura, L. Flamigni and P. Ballester, *Chem.–Eur. J.*, 2011, **17**, 14564.
41 H. Nobukuni, Y. Shimazaki, F. Tani and Y. Naruta, *Angew. Chem., Int. Ed.*, 2007, **46**, 8975.
42 H. Nobukuni, Y. Shimazaki, H. Uno, Y. Naruta, K. Ohkubo, T. Kojima, S. Fukuzumi, S. Seki, H. Sakai, T. Hasobe and F. Tani, *Chem.–Eur.J.*, 2010, **16**, 11611.
43 H.-B. Burgi, E. Blanc, D. Schwarzenbach, S. Liu, Y.-J. Lu, M. M. Kappes and J. A. Ibers, *Angew. Chem., Int. Ed. Engl.*, 1992, **31**, 640.
44 M. Fujiwara, T. Kambe and K. Oshima, *Phys. Rev. B: Condens. Matter Mater. Phys.*, 2005, **71**, 174424.
45 A. O'Neil, C. Wilson, J. M. Webster, F. J. Allison, J. A. K. Howard and M. Poliakoff, *Angew. Chem., Int. Ed.*, 2002, **41**, 3796.
46 D. V. Konarev, A. Yu. Kovalevsky, A. L. Litvinov, N. V. Drichko, B. P. Tarasov, P. Coppens and R. N. Lyubovskaya, *J. Solid State Chem.*, 2002, **168**, 474.

